Molecular Biology of the Cell
Vol. 10, 2309–2327, July 1999

Polymerizing Microtubules Activate Site-directed F-Actin Assembly in Nerve Growth Cones

M. William Rochlin,* Michael E. Dailey,† and Paul C. Bridgman‡

Department of Anatomy and Neurobiology, Washington University School of Medicine, St. Louis, Missouri 63110

Submitted September 2, 1998; Accepted May 3, 1999
Monitoring Editor: Mary C. Beckerle

We identify an actin-based protrusive structure in growth cones termed "intrapodium." Unlike filopodia, intrapodia are initiated exclusively within lamellipodia and elongate in a continuous (nonsaltatory) manner parallel to the plane of the dorsal plasma membrane causing a ridge-like protrusion. Intrapodia resemble the actin-rich structures induced by intracellular pathogens (e.g., *Listeria*) or by extracellular beads. Cytochalasin B inhibits intrapodial elongation and removal of cytochalasin B produced a burst of intrapodial activity. Electron microscopic studies revealed that lamellipodial intrapodia contain both short and long actin filaments oriented with their barbed ends toward the membrane surface or advancing end. Our data suggest an interaction between microtubule endings and intrapodia formation. Disruption of microtubules by acute nocodazole treatment decreased intrapodia frequency, and washout of nocodazole or addition of the microtubule-stabilizing drug Taxol caused a burst of intrapodia formation. Furthermore, individual microtubule ends were found near intrapodia initiation sites. Thus, microtubule ends or associated structures may regulate these actin-dependent structures. We propose that intrapodia are the consequence of an early step in a cascade of events that leads to the development of F-actin-associated plasma membrane specializations.

INTRODUCTION

Protrusion and retraction of filopodia and lamellipodia are critical for both advance and turning of locomoting cells. Movement of the leading edge is a complex process that depends on the orchestration of mechanisms that regulate actin polymerization (Cooper, 1991; Cramer *et al.*, 1994), cross-linking (Oster and Perelson, 1987), contraction by molecular motors (Honer *et al.*, 1988; Mitchison and Kirschner, 1988; Smith, 1988; Rochlin *et al.*, 1995; Lin *et al.*, 1996, Svitkina *et al.*, 1997; Verkhovsky *et al.*, 1999), and cross-linking of the F-actin cytoskeleton to the substratum. To circumvent some of these complexities and learn more about protrusion and F-actin assembly in cells, several groups have focused on the ability of intracellular pathogens or other foreign agents to induce F-actin assemblies in cells. Intracellular pathogens such as *Listeria*, *Shigella*, *Rickettsia*, and the Vaccinia virus (Cossart, 1995; Cudmore *et al.*, 1996; Beckerle, 1998) and extracellularly applied polycation and cell adhesion molecule (CAM) cross-linking beads (Forscher *et al.*, 1992; Suter *et al.*, 1998) induce F-actin assembly-dependent structures that are thought to form as a result of "hijacking" the innate cellular mechanisms involved in protrusion at the leading edge. We now report a spontaneously occurring structure that resembles the F-actin assemblies induced by those foreign agents more closely than do lamellipodia, filopodia, or ruffles. Because this structure is part of the innate motility apparatus of the growth cone, is initiated at a distance from and usually terminates within the growth cone perimeter, we term them "intrapodia."

We have begun to investigate the role of intrapodia in growth cone motility. Although the perimeter of the growth cone has been studied extensively because it is the ultimate site at which changes in direction and advance rate can be regulated, several studies suggest that more proximal regions of the growth cone initiate

Present addresses: *Northwestern University, Department of Neurobiology and Physiology, Evanston, IL 60208; †University of Iowa, Department of Biological Sciences, Iowa City, IA 52242.
‡ Corresponding author.

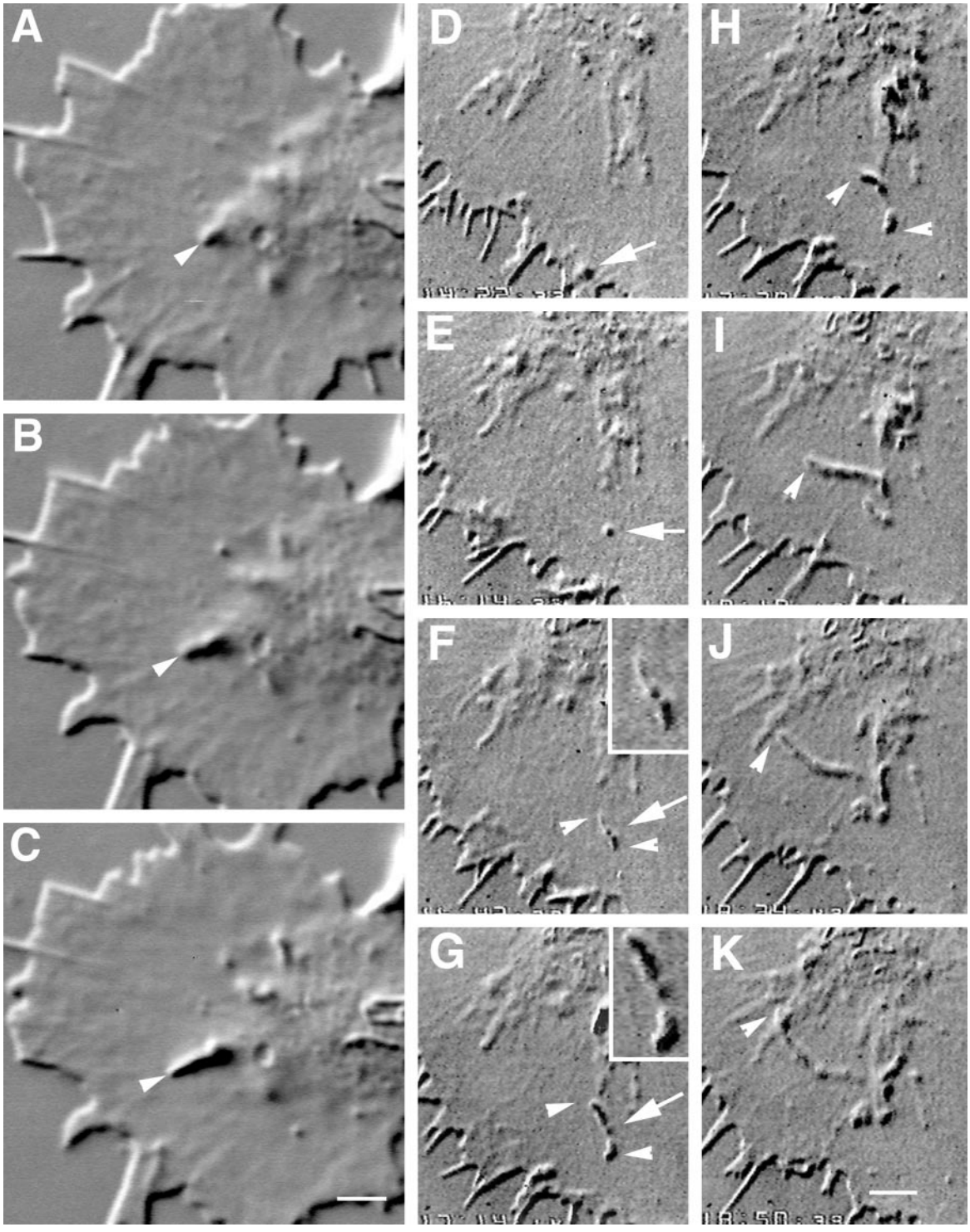

Figure 1. Two time-lapse sequences revealing intrapodia formation and dynamics. (A–C) Intrapodium initiated in the marginal zone. (A) At the onset of intrapodia formation a protuberance is initiated at the margin between the central, organelle-rich domain and the flattened, F-actin-rich domain (arrowhead). In this case, elongation is fairly straight, perhaps because the direction of elongation is orthogonal to the nearest leading edge and therefore is not being "side-swiped" by the retrograde flow. A second intrapodium is developing near the top. Time interval between images is 5 s. (D–K) Intrapodia that developed in the peripheral domain of a growth cone from a particle released from the leading edge and carried rearward by the retrograde flow. (D) Just after release of a particle from the leading edge (arrow). During the rearward movement, but before E, the particle increases in length but then shortens to assume its original size (our unpublished results).

the series of events that lead to these changes. In particular, microtubules that terminate proximally within lamellipodia appear capable of inducing growth cone turning (Tanaka and Kirschner, 1991, 1995; Tanaka and Sabry, 1995; Suter *et al.*, 1998), and manipulations that perturb microtubule dynamics interfere with advance (Tanaka *et al.*, 1995; Rochlin *et al.*, 1996) and turning (Williamson *et al.*, 1996). One mechanism by which microtubules could exert these effects is by stabilizing sites at which the plasma membrane attaches to the substratum (Rinnerthaler *et al.*, 1988; Bershadsky *et al.*, 1996; Kaverina *et al.*, 1998). Interestingly, two cues that stimulate the formation of attachment specializations first stimulate protrusive F-actin assembly: CAM cross-linking beads (Suter *et al.*, 1998) and growth factors (Hall, 1998). Microtubules are also implicated in stimulating F-actin assembly at the leading edge of non-neuronal cells (Vasiliev and Gelfand, 1976; Rinnerthaler *et al.*, 1988; Bershadsky *et al.*, 1991; Rosania and Swanson, 1996; Waterman-Storer *et al.*, 1999). Given that most microtubules within the growth cone terminate in the proximal region where intrapodia are most likely to be initiated, we evaluated the relationship between microtubule polymerization and intrapodia formation. Our results suggest that microtubule polymerization triggers intrapodia initiation, and that this event precedes microtubule-based stimulation of protrusion at the leading edge.

MATERIALS AND METHODS

Fetal rat superior cervical ganglion explant (SCG) cultures were prepared as described previously and grown on laminin-coated coverslips (Rochlin *et al.*, 1995). Just before observation the coverslips was mounted in a perfusion chamber (Berg and Block, 1984). The chamber design permits simultaneous differential interference contrast (DIC) observation and perfusion. Growth cones were imaged by video-enhanced DIC microscopy. The microscope field was illuminated intermittently by a 100-W mercury lamp for purposes of time-lapse recording or for focus adjustment. At the end of some sequences, the chamber was perfused with PHEM buffer (60 mM PIPES, 25 mM HEPES, 10 mM EGTA, and 2 mM $MgCl_2$, pH 6.9) (Schliwa *et al.*, 1981) containing glutaraldehyde (0.25%; EM Science, Fort Washington, PA), saponin (0.02%; Sigma, St. Louis, MO), and rhodamine-phalloidin (80 nM; Molecular Probes, Eugene, OR; or Sigma). After a 15- to 20-min incubation, fluorescence images were collected using a slow scan, cooled charge-coupled device (Photometrics, Tucson, AZ) and stored as $512 \times 512 \times 16$-bit digital image files. If antibody staining was to be carried out on these cultures, they were treated with 1% OsO_4 in PBS at 4°C for 5 min, washed extensively in PBS at room temperature, treated with freshly prepared 5% β-mercaptoethanol (Pierce, Rockford, IL) at room temperature for 30 min, washed extensively, and blocked for 15–30 min with 8 mg/ml BSA, 0.5% fish gelatin (Amersham, Arlington Heights, IL), and 1% normal goat serum in PBS. We stained with the primary antibodies for 1 h and the secondary antibodies for 40 min at room temperature. Primary antibodies were used at 1:1000 (mouse anti-β-actin; Sigma), 1:200 (rabbit anti-β_1-integrin, generously provided by Dr. L. Reichardt, University of California, San Francisco, CA), and 1:100 (rat anti-tyrosinated tubulin; Accurate Scientific, Westbury, NY). Low–cross-reactivity secondary antibodies were obtained from Jackson ImmunoResearch (West Grove, PA) and used at 1:800 (Cy3 goat anti-rabbit), 1:400 (fluorescein goat anti-mouse), and 1:800 (Cy5 goat anti-rat).

For electron microscopy (EM), cultures were observed by DIC microscopy and fixed during intrapodia formation as described above for phalloidin staining. However, immediately after completion of perfusion of the PHEM buffer containing saponin and phalloidin, we perfused with PHEM buffer containing 0.7% Triton X-100 (Pierce) and 2% glutaraldehyde. Some cultures were perfused with 1 mg/ml myosin S1 in PHEM buffer for 10 min, rinsed briefly with buffer, and fixed as above (Lewis and Bridgman, 1992). To preserve actin structure, cultures were first treated with tannic acid and uranyl acetate as described by Svitkina and Verkhovsky, (1995) and then critical point dried and rotary shadowed. The growth cones observed in DIC recordings were relocated in the replicas on slot grids using a Jeol (Tokyo, Japan) 1200EX transmission electron microscope. Some EM images were digitized directly from the negative using an Agfa (Mortsel, Belgium) Duoscan scanner operating at maximum resolution and dynamic range.

Net extension rates of intrapodia were determined by measuring the final length of intrapodia before fixation or at their maximal length, whichever came first, and dividing by the number of seconds that separated initiation of outgrowth from attainment of the maximal length. To measure changes in the area of the leading margin of the growth cone, DIC images were digitized at 1.5-min intervals and magnified sufficiently to allow accurate tracing of the growth cone perimeter. The leading 50% of the growth cone area was analyzed. Pairs of consecutive images were overlaid, regions of protrusion and retraction were identified, and their areas were quantitated and the net changes in area were determined.

We also evaluated the correspondence of the direction of intrapodial growth with the direction of growth cone advance. Perpendicular intrapodial growth was defined as a growth direction that fell within 6° of perpendicular to the most recently deposited 5 μm of neurite shaft. Forward or reverse growth was simply defined as the 168° distal to or proximal to, respectively, the perpendicular growth zone.

Drug treatments were performed by perfusing drug-containing media through the recording chamber during DIC observation. A heat lamp was used to ensure that the media was kept at 37°C before and during perfusion. Cytochalasin B was used at concen-

Figure 1 (cont). (E) The particle (arrow) continues to move rearward, carried back by the retrograde flow. (F) Two intrapodia extend away from the particle (arrowheads, see inset), growing in opposite directions. (G) Intrapodial growth continues, but the direction of growth begins to curve to the left. The intrapodium that initially grew toward the center of the growth cone (proximal intrapodium) elongates more rapidly than the intrapodium that initially grew toward the leading edge (distal intrapodium) against the retrograde flow. (H) The distal intrapodium appears to have discontinued net extension in the plane of the growth cone, whereas the proximal intrapodium continues to extend, now in a direction parallel to the leading edge and perpendicular to its original direction. (I) The proximal intrapodium (arrowhead) continues to grow in the same direction. The distal intrapodium grows much less and appears to be meandering. (J) The proximal intrapodium continues to extend toward linear elements emanating from the central region of the growth cone. These linear elements presumably contain microtubules and endoplasmic reticulum and vesicular structures known to extend along microtubules in peripheral regions of growth cones (Dailey and Bridgman, 1991). (K) A large portion of the tail is dissolved, leaving behind a few remnants. The tip of the proximal intrapodium continues to advance, but upon contacting the linear elements, it turned abruptly, coursing centripetally along the linear structure. Bar, 5 μm.

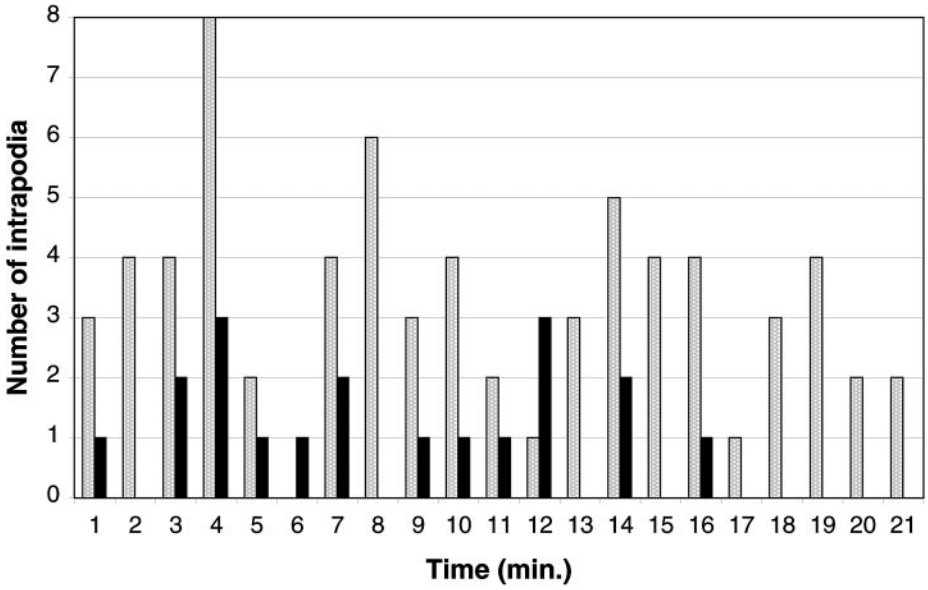

Figure 2. Histogram of intrapodia frequency in growth cones elongating exclusively on the laminin-coated coverglass (solid bars) or along a neurite (stippled bars). The number of intrapodia observed in 1-min intervals is plotted. In both situations, intrapodia frequency is episodic. The level of intrapodia activity is higher in the growth cone elongating along another neurite.

trations ranging from 0.06 to 5 μM, and nocodazole was used at concentrations ranging from 0.33 to 6.6 μM.

Digital images were adjusted and prepared as composites using Adobe (Mountain View, CA) Photoshop and printed using a Tektronix (Wilsonville, OR) dye sublimation printer.

RESULTS

Characterization of Intrapodia

Intrapodia Formation. Rat SCG growth cones grown on laminin substrates typically are well spread, relatively thin, and highly motile. They contain two distinct cytoplasmic domains, a thickened organelle and microtubule-rich central domain and a thin actin-rich peripheral domain (Bridgman and Dailey, 1989). Intrapodia most often form at the margin between the peripheral and central domains (Figure 1, arrowheads), but are also initiated within lamellipodia. For the purposes of quantitation we defined the marginal zone as a 4-μm-thick strip separating the thin lamellipodium from the thicker central region. Fifty-seven percent of the intrapodia (n = 185) formed in the marginal zone (from recordings of four cones). Most of the remaining intrapodia formation (38%) occurred within lamellipodia. On occasion, we observed the formation of an intrapodium from a particle that appeared to have been part of the leading edge (Figure 1, D–F). Particles were observed only in very well spread cones with extremely thin lamellipodia; thus it was not possible to accurately quantitate the percentage of intrapodia that formed from particles. In growth cones observed 16–24 h after plating (and not making contact with adjacent cells), the average frequency of formation was 1.0 ± 0.4 (SD) intrapodia/min (n = 8; from 20-min recording time per cone). Intrapodia tended to form in bursts of two to four with irregular intervals between bursts (Figure 2). The average frequency of intrapodia formation increased to 4.9 ± 0.46 intrapodia/min (n = 5; 20-min recording time for each) in growth cones adhering to and growing along adjacent neurites (e.g., Figure 2), indicating that environmental factors influence the rate of intrapodia formation. Because of the variation in individual rates of intrapodia formation between cones, we also compared a set of cones before and after contact and turning toward neighboring neurites. This set of cones showed a rate of intrapodia formation of 1.9 ± 0.8/min before contact that increased to 4.0 ± 1.6/min after contact (N = 5; 5–10 min before contact and 10 min after contact). The increased formation of intrapodia in cones contacting neurites occurred in the marginal zone and new regions of lamellipodia that formed as the cone reoriented its trajectory by spreading in a direction approximately parallel with the long axis of the neurite that it contacted.

Growth Rate and Trajectory of Intrapodia. Intrapodial profiles extended at an average rate of 0.18 ± 0.01 (SEM) μm/s (n = 18). This rate is approximately the same as that reported by Forscher *et al.* (1992) for the retrograde flow-corrected rate of bead displacement by "inductopodia" and also the rate of Arp3/capping protein "spots" in a variety of non-neuronal cells types (Schafer *et al.*, 1998). Intrapodia net extension rates ranged from 0.10 to 0.32 μm/s. Typically, intrapodia extension took a curvilinear path. The paths curved smoothly unless the leading tip of the intrapodium encountered another structure within the cytoplasm.

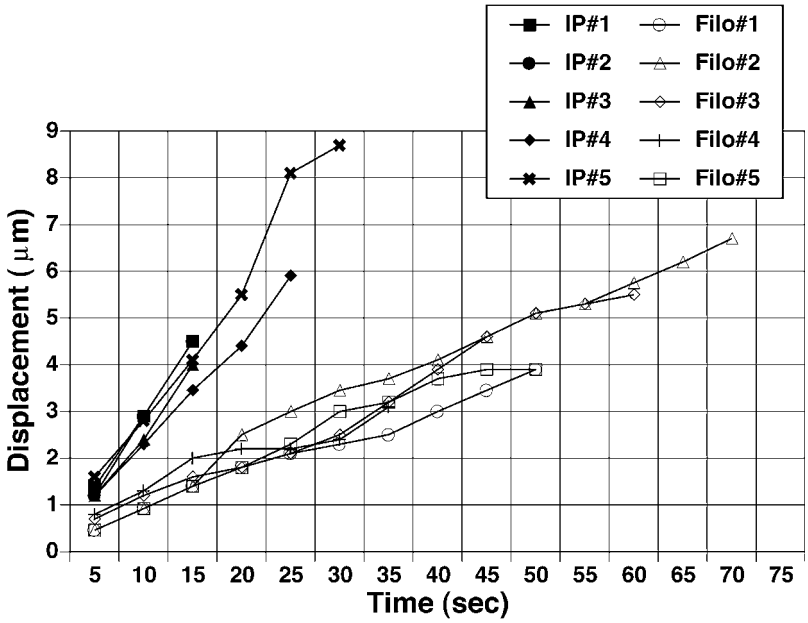

Figure 3. Comparison of elongation of individual intrapodia (IP) and filopodia (Filo). Intrapodia elongate more rapidly than filopodia. This is due in part to the saltatory nature of filopodial growth and also to a slower elongation rate during periods of growth.

In one sequence we observed intrapodium travel in one direction (Figure 1, I and J) until its tip encountered a linear element, perhaps a microtubule. After contact, the intrapodium abruptly changed direction and advanced along the linear element (Figure 1K). These observations are consistent with the possibility that intrapodia are propelled from the rear, changes in their direction resulting from changes in resistance encountered at the front. Occasionally, intrapodia arising from the central thickened region of the growth cone would extend toward the leading edge, punching outward to create filopodia-like protrusions, or extending along previously formed filopodia (our unpublished observation). Finally, we also observed intrapodia that curved sharply and then disappeared coincident with the formation of endocytotic vacuoles (see Dailey and Bridgman, 1993, their Figure 12). These vacuoles were also observed to form without detectable intrapodial activity, but the coincidence of their occurrence with the disappearance of intrapodia suggests a relationship.

We also assessed the direction of intrapodial advance in relation to the direction of growth cone advance. In a rapidly advancing growth cone over a 40-min period, 80% of the intrapodia elongated forward along the axis of growth, 10% elongated perpendicular to this axis, and the remaining 10% elongated antiparallel to this axis. This suggests that intrapodia may preferentially elongate in the direction of growth cone advance.

Comparison with Filopodia. For comparison, we gathered rate and persistence data on filopodia. Filopodia extended slower (0.13 ± 0.04 [SEM] μm/s; n = 7) than intrapodia, and this growth was more frequently interrupted by periods of stasis (Figure 3). Also, the average lifetime of intrapodia (1.5 min; n = 33) was significantly less than that of filopodia (7.8 min; n = 9). Finally, at their peak lengths, filopodia are longer (8.0 ± 3.2 [SD] μm; n = 25), on average, than intrapodia (4.9 ± 2.1 μm; n = 20). Note that it was not possible to assess these properties for filopodia that projected upward (away from the substratum) because of the difficulty of tracking out-of-focus filopodial tips. However, we did determine the lifetime of ruffles (sheet-like and filopodial-like) for comparison. The average lifetime of these structures was 3.6 ± 1.9 (SD) min (n = 10).

Intrapodia Contain F-Actin and F-Actin-binding Proteins. To determine whether intrapodia contain F-actin, we stained growth cones with rhodamine-phalloidin. Upon seeing the formation of an intrapodium during live observations (Figure 4, A–C), we perfused the chamber with fixative (Figure 4D) followed by saponin and rhodamine-phalloidin (Figure 4H). Intrapodia were always associated with intense phalloidin staining, indicating that F-actin is concentrated in intrapodia compared with surrounding cytoplasm. We also labeled growth cones with anti-β-actin to ascertain whether pools of G-actin were associated with intrapodia but found no difference from the phalloidin labeling (our unpublished observation). We investigated whether actin-binding proteins that are associated with actin–plasma membrane linkage sites were present in intrapodia. The brightness of talin and α-actinin immunofluorescence staining was greater along the length of intrapodia (our unpublished observation), as was the staining for β_1-integrin subunit (Figure 4, E and F). At the light micro-

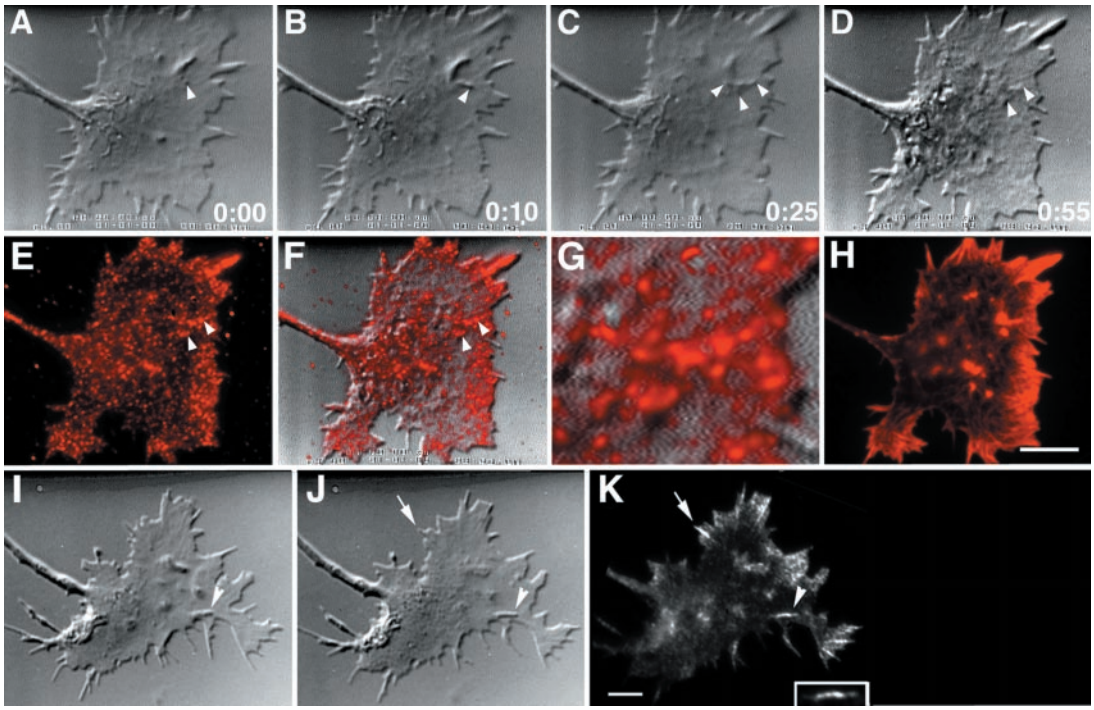

Figure 4. Intrapodia are composed of F-actin and F-actin-associated proteins. Growth cones were fixed during live observation and stained for actin, β_1-integrin, or capping protein. (A–K) A growth cone stained for actin and β_1-integrin. (A–D) DIC images of growth cone before and after fixation (time is in seconds). (A) The intrapodium (arrowhead) is initiated in the marginal zone. (B) The tip of the intrapodium advances toward the leading edge, against the direction of the retrograde flow. (C) Moments before the arrival of the fixative, but during perfusion, the intrapodium continues to elongate toward the leading edge. In addition, two smaller intrapodia have begun to form nearby, one extending toward the central, thickened region of the growth cone and the other extending tangential to the marginal zone. Because of the perfusion, the focus drifts slightly. (D) After completion of fixation, the growth cone is thinner, but there is sufficient contrast to resolve the two intrapodia that were closest to the leading edge. (E) β_1-Integrin staining is elevated along intrapodia (arrowheads) and also along the leading edge. (F) Overlay of β_1-integrin staining on the DIC image of the fixed growth cone in D, showing the coincidence of the elevated integrin staining and the intrapodia (arrowheads). (G) 4× zoom of F, featuring the growth cone region containing the intrapodium. Note that the β_1-integrin staining is punctate along the intrapodia. (H) Before immunostaining, the growth cone was labeled with rhodamine-phalloidin. Bar, 9 μm. (I–K) Growth cone stained for capping protein (Schafer *et al.*, 1998). Capping protein staining was distributed along the length of the intrapodium (arrowhead) and also stained rib-like structures that presumably correspond to F-actin bundles that are perpendicular to the leading edge (arrow). Inset, colocalized capping protein staining (2× zoom). Bar, 5 μm.

scopic level, the leading tips were not more intensely labeled for any of these antigens than along the rest of the length of the intrapodium. Capping protein was concentrated along the length of intrapodia (Figure 4, I–K, arrowhead) as well as along actin bundles in lamellipodia that impinged on the leading edge (Figure 4K, arrows). Because capping protein binds to the barbed end of F-actin, this indicates that capped barbed ends are staggered along the length of these bundles. Comparison of the average pixel brightness within intrapodia with that of the surrounding lamellipodium indicated a greater than threefold difference (3.6 ± 0.9 [SD]; $n = 5$) in capping protein staining intensity.

Electron Microscopic Observations Confirm the Presence of a High Concentration of Actin Filaments within Intrapodia. To study intrapodial ultrastructure, growth cones were extracted and fixed during DIC observation of intrapodial activity, processed for electron microscopic observations, and reidentified (see MATERIALS AND METHODS). Stereo EM images of rotary-shadowed cytoskeleton preparations allowed the observation of intrapodial actin filament organization (Figure 5). Intrapodia contained a dense network of actin filaments that created a ridge on the dorsal surface of the growth cone. Many of the filaments within the ridge were oriented approximately parallel to the long axis of the intrapodium. Surface replicas of the dorsal membrane surface prepared by freeze etch EM also confirmed that intrapodia formed a ridge in unextracted preparations (our unpublished observation). We estimated the relative thickness of these ridges compared with that of the lamellipodium by viewing stereo pairs in a parallax measuring device. Although variable in height, the ridges were on average about twice the thickness of lamellipodia (1.8 ± 0.96 [SD] μm; $n = 5$). Thus, the thickness, density, and orientation of filaments within the lamel-

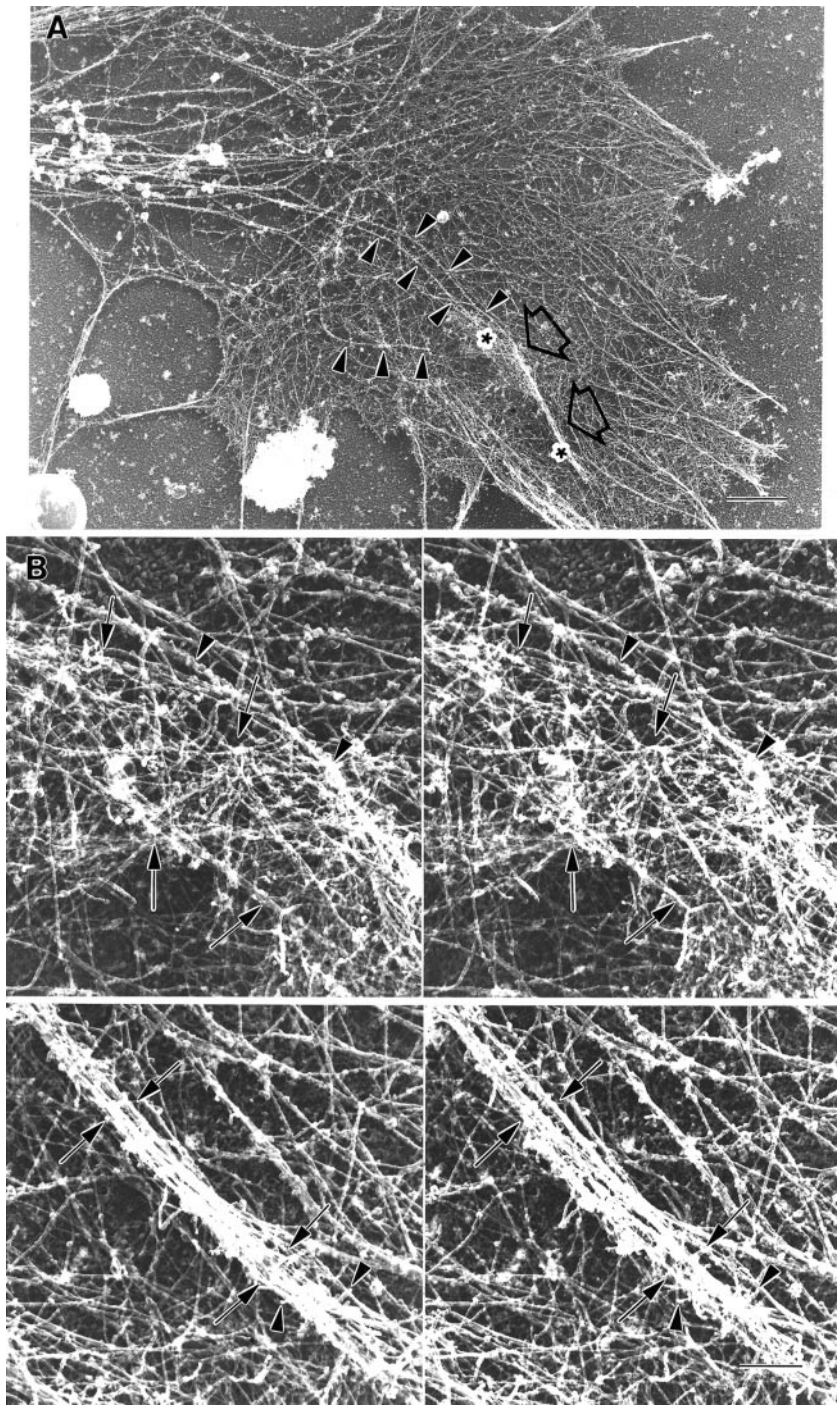

Figure 5. Electron micrograph of a growth cone–containing intrapodia reveals deformation of dorsal plasma membrane, a high concentration of actin filaments, and microtubule endings. (A) Low-magnification EM image of a rotary-shadowed growth cone cytoskeleton. An intrapodium (large arrows) that was identified and tracked by video-enhanced DIC recording (our unpublished data) before fixation and extraction of the membrane elongated from a region in close proximity to the ends of microtubules (arrowheads). (B) Higher-magnification stereo pairs of the two areas indicated by the asterisks in A. The first area contains the origin of the intrapodium. A relatively broad, dense mass of actin filaments (between the arrows) forms a ridge on the dorsal surface of the cone. A microtubule (arrowheads) that appears decorated with globular material ends on one side of the ridge (the microtubule end is adjacent to the arrowhead on the right). The second area contains the leading end of the intrapodium. A bundle of actin filaments forms a narrow ridge (between arrows). At the tip of the intrapodium, numerous filament ends can be seen (arrowheads). Bars, 2.6 μm (A); 360 nm (B).

lipodium were focally changed by the complex network of actin filaments that make up the intrapodium. Near the leading tip of intrapodia, filaments from the lamellipodium that coursed tangential to the ridge formed by the intrapodium appeared to be pushed dorsally. It could not be determined whether these filaments were integrated into the intrapodial actin network or whether they were being pushed upward by the advancing intrapodia. The base (or trailing end) of an intrapodium was broader and flatter than the tip. F-actin at the trailing end and ventral-most portion of the ridge was integrated into the adjacent actin cytoskeleton through a complex branching network of filaments. Such a relationship has not been reported

for intracellular pathogens (Cossart, 1995; Cudmore *et al.*, 1996).

Along the length of intrapodia, free filament ends could be seen oriented with their tips upward (toward the dorsal surface). Filament ends appeared more concentrated at the tip. It was difficult to determine the length of actin filaments because of the high density and complex geometry, but the general impression was that both long and short filaments contributed to the meshwork that formed the ridge. Longer filaments oriented tangential to the long axis of intrapodia were observed along the sides of intrapodia but could not be unambiguously identified within the core of these dense structures. Katoh *et al.*, (1999) recently reported that intrapodia in *Aplysia* growth cones also contain longitudinally oriented F-actin. The mixture of lengths of F-actin in intrapodia is more reminiscent of the ultrastructure of *Rickettsia* (Heinzen *et al.*, 1993) and Vaccinia tails (Cudmore *et al.*, 1996) than of *Listeria* tails (Tilney *et al.*, 1992a,b; but see Zhukarev *et al.*, 1995; Sechi *et al.*, 1997). The polarity of some of the F-actin filaments within the intrapodium could be determined (Figure 6). Using stereo images taken at three different tilt angles (+10, 0, and −10°) we were able to determine the orientation of 30 filaments from three different intrapodia that were previously observed by DIC microscopy to elongate. We divided the filaments into two categories; those aligned parallel to the long axis of the intrapodium and those oriented perpendicular to the overlying membrane (parallel with the z-axis). Ninety-five percent of the filaments that were parallel to the long axis had their barbed ends oriented toward the advancing intrapodium tip. Seventy-eight percent of the filaments aligned along the z-axis were oriented with their barbed ends toward the dorsal membrane surface. We also identified an additional five intrapodia on the basis of their characteristic morphology in the same replicas. When we analyzed the orientation of filaments in these intrapodia, the results were similar: 94% of the filaments parallel to the long axis of the intrapodia were oriented with their barbed ends toward the tip, and 92% of the filaments aligned along the z-axis had their barbed ends oriented toward the dorsal membrane surface. We have not consistently observed evidence for a particle or vesicle at the tip of these structures.

Intrapodial Particle Formation and Tip Advance Appear to Be Differentially Sensitive to Cytochalasin B. Given the accumulation of F-actin in the tails of intrapodia, we tested whether the formation of the advancing tip was inhibited by cytochalasin B (see MATERIALS AND METHODS). Intrapodia did not form during high (≤2.5 μM) cytochalasin treatment. Latrunculin B (20 nM), a toxin derived from the Red Sea sponge, binds to G-actin (Spector *et al.*, 1989) and had similar effects (our unpublished observation). These treatments appeared to cause a rapid thinning of lamellipodia, loss of a coherent retrograde flow, accumulations of cytoplasm into thickened islands (Figure 7), and an increase in the frequency of random particle trajectories (Evans and Bridgman, 1995). The leading edges remained thick, retracted only slightly, and never extended. We did not observe the en masse retrograde evacuation of cytoplasmic materials that was beautifully captured by Forscher and Smith (1988) in *Aplysia* growth cones treated with cytochalasin B.

After washout of the cytochalasin, we typically observed a flurry of intrapodial formation (Figure 7, C and D), even in growth cones in which no intrapodia had been detected during precytochalasin observation. On average, we observed 11 ± 4 intrapodia per 1.5 min before cytochalasin treatment, 24 ± 6 during the first 1.5 min after cytochalasin washout, and 15 ± 3 during the subsequent 1.5 min period ($n = 5$). The burst of intrapodial activity was significantly greater than the precytochalasin level ($p < 0.0015$) and that of the subsequent 1.5-min period ($p < 0.005$). This observation is consistent with cytochalasin inducing the formation of intrapodia initiators but blocking intrapodial extension. The burst of intrapodial activity after cytochalasin washout was superimposed on rapid recovery of lamellipodial thickness and an increase in protrusive activity at the leading edges.

How might intrapodial activity be induced by cytochalasin treatment and washout? By viewing our time-lapse images in reverse, we observed that evacuation of cytoplasm from lamellipodia was also accompanied by the intermittent retrograde transport of particles that appeared to be breaking off from the leading edge. These particles typically ended up in the cytoplasmic islands that were the site of intrapodial activity after cytochalasin washout and may therefore contribute to the burst of intrapodial activity. Also, phalloidin or anti-β-actin staining of cytochalasin-treated growth cones revealed foci of brightly staining actin in these islands and also along F-actin bundles that were resistant to the cytochalasin treatment. We suspect that these actin-rich particles are intrapodia initiators and that they seed intrapodia after cytochalasin washout.

Influence of Microtubules on Intrapodia Formation

Nocodazole Alters the Formation Rate of Intrapodia. Although actin and actin-binding proteins are thought to be the primary effectors of growth cone shape and dynamics, perturbations of microtubules have been shown to affect pseudopodial dynamics in a variety of systems (Vasiliev and Gelfand, 1976; Tanaka *et al.*, 1995; Rosania *et al.*, 1996). We therefore examined the influence of nocodazole on intrapodial frequency.

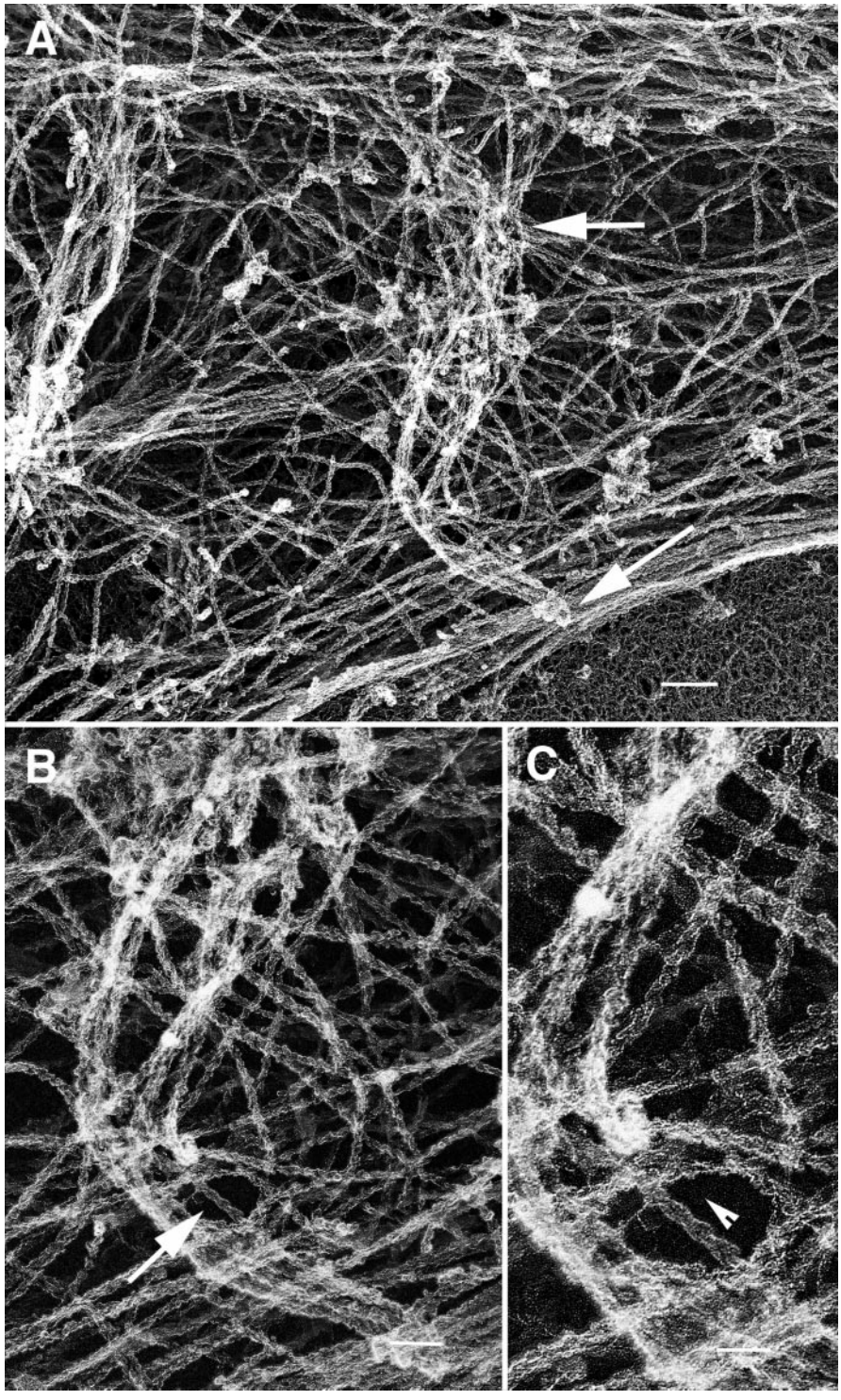

Figure 6. Polarity of actin filaments observed using myosin S1 decoration. (A) An intrapodium extends from its base (upper arrow) toward the cell margin (lower arrow). (B) Decorated filaments in the intrapodium (arrow) are superimposed upon those in the underlying lamellipodia. Stereo images of this intrapodium (our unpublished data) allowed identification of intrapodial-associated filaments. (C) A higher magnification allows the decorated filament orientation (indicated by the arrowhead) to be seen in a small portion of intrapodium-associated filaments. Bars, 360 nm (A); 180 nm (B); 90 nm (C).

During live observation, we perfused the cultures with 3.3 or 6.6 μM nocodazole, two concentrations that we previously established to eliminate microtubules from the growth cone in <30 min (Rochlin *et al.*, 1996). These treatments decreased intrapodia frequency (Figure 8A). We also observed that filopodial and lamellipodial protrusion and growth cone advance were decreased (our unpublished observation). Compared with intrapodia in untreated growth cones, intrapodia in nonadvancing growth cones in 3.3 μM

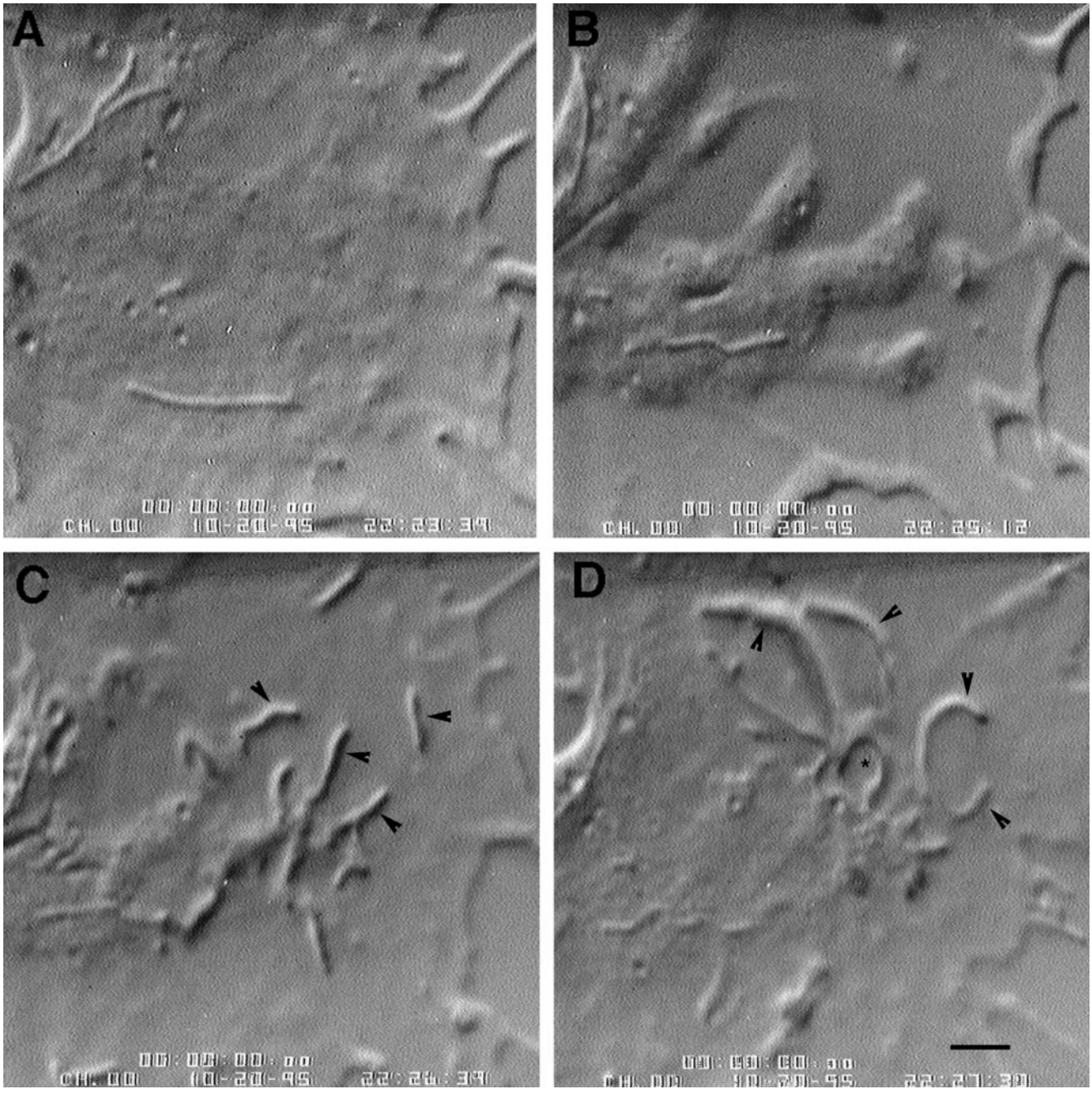

Figure 7. Cytochalasin B washout causes a burst of intrapodial activity. In this case the SCG explant had been plated and maintained in a low dose of nocodazole. (A) Just after perfusion with cytochalasin. (B) One minute 33 s later. Note the more flattened appearance of the lamellipodium, the thickened leading edge, and the islands of cytoplasm that accumulate in the lamellipodium. (C and D). After perfusion of cytochalasin-free media. In this instance, intrapodia (arrowheads) emanated from one cytoplasmic island, producing a starburst appearance. Bar, 5 μm. *, Reverse shadow-cast vacuole.

nocodazole elongated with considerably less bias toward the leading edge of the growth cone. Only 44% elongated toward the forward axis (vs. 80% in untreated cultures), and 24% elongated in the opposite direction (vs. 10% in untreated cultures). Growth cones recovered from washout of the 3.3 μM nocodazole, but the disruption caused by 6.6 μM treatments did not appear reversible during the time course of our observations.

We also tested the influence of lower doses of nocodazole on intrapodial frequency. Explant cultures were

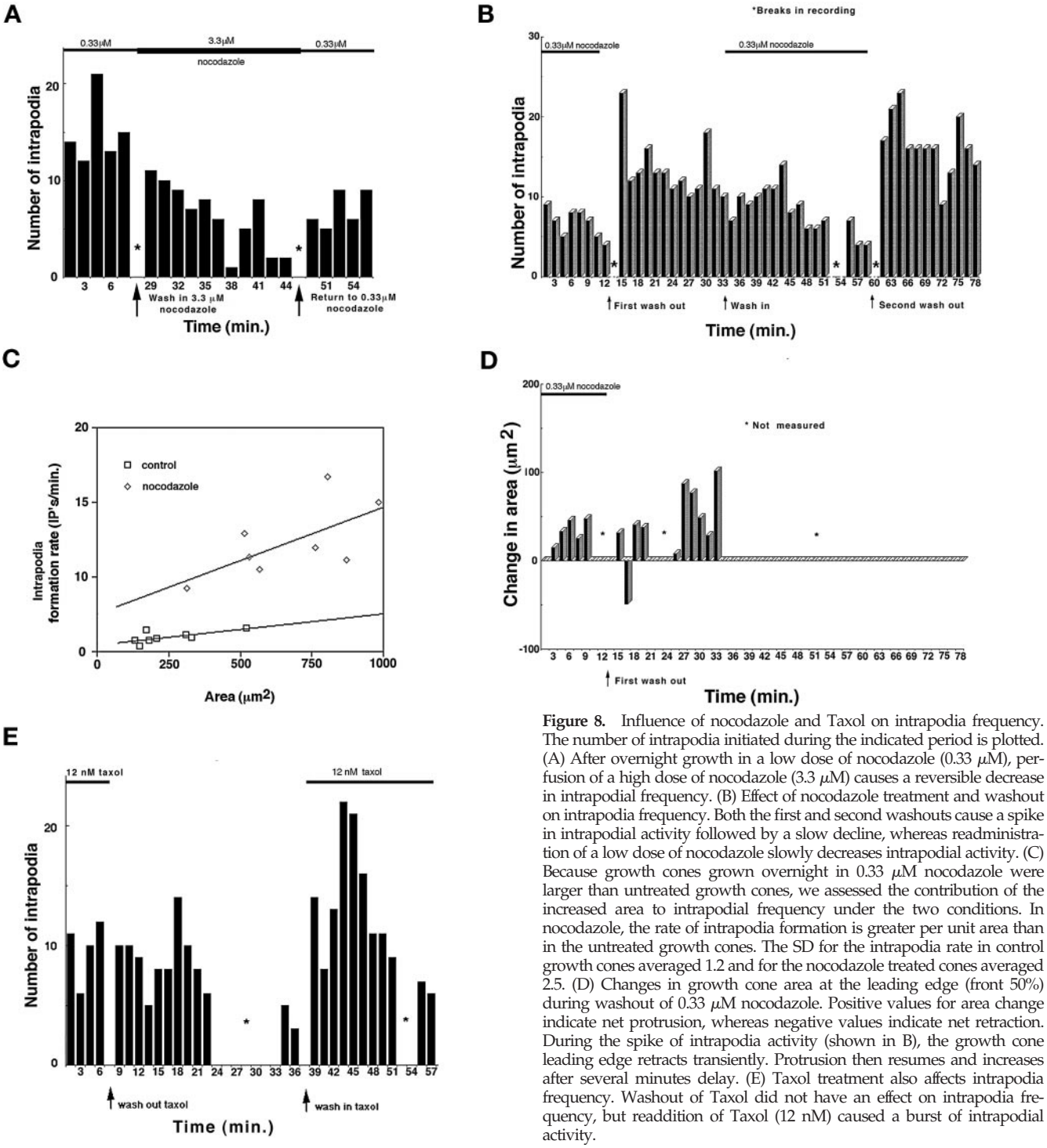

Figure 8. Influence of nocodazole and Taxol on intrapodia frequency. The number of intrapodia initiated during the indicated period is plotted. (A) After overnight growth in a low dose of nocodazole (0.33 μM), perfusion of a high dose of nocodazole (3.3 μM) causes a reversible decrease in intrapodial frequency. (B) Effect of nocodazole treatment and washout on intrapodia frequency. Both the first and second washouts cause a spike in intrapodial activity followed by a slow decline, whereas readministration of a low dose of nocodazole slowly decreases intrapodial activity. (C) Because growth cones grown overnight in 0.33 μM nocodazole were larger than untreated growth cones, we assessed the contribution of the increased area to intrapodial frequency under the two conditions. In nocodazole, the rate of intrapodia formation is greater per unit area than in the untreated growth cones. The SD for the intrapodia rate in control growth cones averaged 1.2 and for the nocodazole treated cones averaged 2.5. (D) Changes in growth cone area at the leading edge (front 50%) during washout of 0.33 μM nocodazole. Positive values for area change indicate net protrusion, whereas negative values indicate net retraction. During the spike of intrapodia activity (shown in B), the growth cone leading edge retracts transiently. Protrusion then resumes and increases after several minutes delay. (E) Taxol treatment also affects intrapodia frequency. Washout of Taxol did not have an effect on intrapodia frequency, but readdition of Taxol (12 nM) caused a burst of intrapodial activity.

maintained in 0.33 μM nocodazole, a concentration that decreases the dynamic instability of microtubule plus ends without causing depolymerization (Jordan *et al.*, 1993). Chronic treatment with 0.33 μM nocodazole resulted in an elevated frequency of intrapodia formation (Figure 8B). Because these growth cones were larger on average than control growth cones, we determined the frequency of intrapodia formation per unit area (Figure 8C). The frequency of intrapodia per unit area was also increased in nocodazole-treated cultures, suggesting that

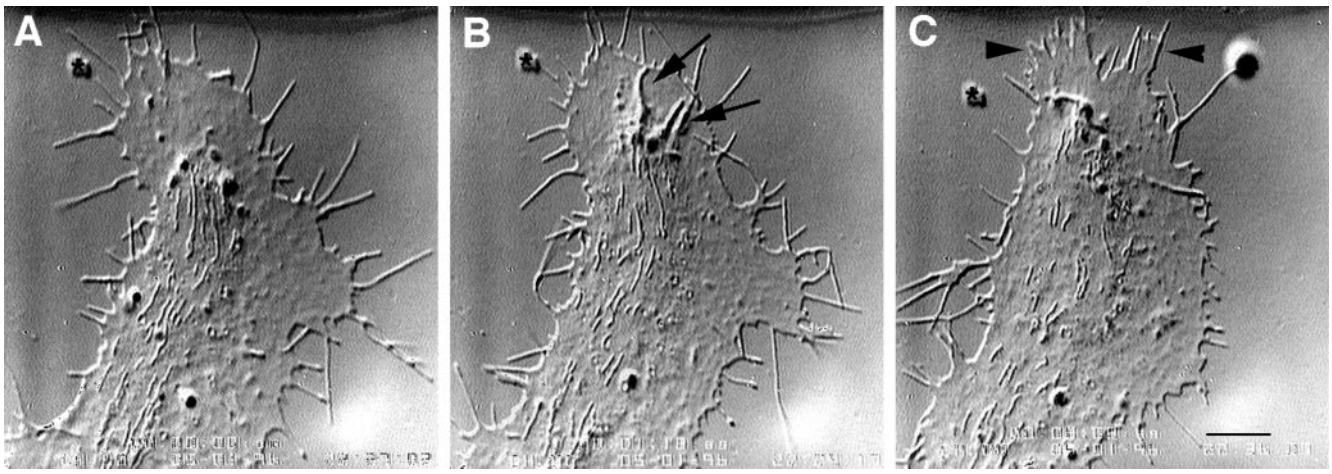

Figure 9. Nocodazole washout causes a burst of intrapodial frequency followed by leading edge protrusion. (A) Before washout of 0.33 μM nocodazole. (B) Just after washout (1 min, 18 s). Note the intrapodia (arrows) that formed at the edge of the marginal zone and elongated toward the leading edge. Protrusion at the leading edge is minimal compared with A. (C) Protrusion at the leading edge (arrowheads) is now observed (8 min, 8 s after washout). Bar, 7 μm.

the increase in frequency was not simply due to the growth cones being larger.

Surprisingly, washout of the 0.33 μM nocodazole resulted in a burst of intrapodial activity (Figures 8B and 9). In contrast, the leading edge initially retracted (coincident with the initial burst of intrapodia activity) (Figure 8D). Leading edge protrusion then resumed and increased (compared with that seen in nocodazole) after several minutes delay, as intrapodia frequency declined (Figure 8, B and D). Filopodia formation before washout (10 $\pm$ 2 per 1.5 min; n = 4) was not significantly different from the rate of formation during the 1.5 min just after washout (10 $\pm$ 4) or during the subsequent 1.5 min (8 $\pm$ 2). Finally, we also observed an increase in the rate of neurite formation at the base of the growth cone after the washout (our unpublished observation). These effects were reversible and repeatable on the same growth cone. Perfusion of medium containing the same concentration of nocodazole used for overnight growth (0.33 μM) had no effects on intrapodia frequency or leading edge protrusion.

Our previous work (Rochlin *et al.*, 1996) (cf. Tanaka *et al.*, 1995) established that washout of nocodazole resulted in lengthening of microtubules in the growth cone and presumably a resumption of normal dynamic instability. To determine whether the changes in intrapodial activity after alterations in nocodazole level were more likely due to changes in dynamic instability or in lengthening of microtubules, we next investigated the influence of Taxol treatment on intrapodia formation.

Taxol Alters Intrapodia Formation Rate. Taxol, like nocodazole, decreases the rate of rapid polymerization events and catastrophe among populations of microtubules (Jordan *et al.*, 1993). In contrast to nocodazole, Taxol promotes assembly of microtubules. In explant cultures grown overnight in low doses (7 or 12 nM) of Taxol, neurite outgrowth length decreased to 80% (n = 5) and 50% (n = 6), respectively, of the control rate of growth. As was the case for nocodazole-treated cultures, neurites were thicker, suggesting that the presence of Taxol did not decrease the rate of axoplasm production. In contrast to cultures grown in nocodazole, extremely large growth cones were not observed in the presence of Taxol. Intrapodial formation rate also appeared elevated in these cultures compared with controls (our unpublished observation, but compare Figure 8E before washout with the control rates stated above in Intrapodia Formation. Washout of Taxol did not elicit an elevation in intrapodia frequency. However, perfusing Taxol-containing media through the chamber resulted in a burst of activity similar to that observed after washout of nocodazole (Figure 8E). Because washout of nocodazole and perfusion of Taxol would be expected to have opposite effects on microtubule dynamic instability, but both treatments would be expected to increase microtubule polymerization, our data suggest that microtubule polymerization, rather than a change in dynamic instability per se, is capable of increasing intrapodial frequency. We next examined whether microtubule endings were located near sites of intrapodia initiation.

Microtubule Endings Are Found near Some Sites of Intrapodia Initiation. To establish whether microtubule endings are present at sites of intrapodia initiation, we fixed growth cones during live observation of intrapodia formation. We attempted to fix growth

cones just at the time that intrapodia were developing. For control growth cones, fixation was initiated at the time intrapodia first became discernible (Figure 10, A and D). We also fixed growth cones just after washout of nocodazole (Figure 10, B and E) or perfusion of Taxol-containing media (Figure 10, C and F). In all three conditions, it appeared that microtubule endings were often at the sites of initiation of intrapodia. We then determined whether this association could result from random colocalization. The association was significantly greater than would be predicted by random distributions of microtubules and intrapodia in four growth cones in which microtubule polymerization was stimulated pharmacologically ($p < 0.06$; Table 1). In two untreated growth cones, we did not detect a nonrandom relationship between microtubule endings and intrapodia. Electron microscopic observations corroborated an association between microtubule endings and the sites of intrapodia initiation (Figure 5). Because of the high density of actin, we could not ascertain whether cytoskeletal elements connected the microtubule endings directly to the actin network within intrapodia. Microtubule polymerization is neither necessary nor sufficient for intrapodia formation, because intrapodia are sometimes observed to form in regions apparently devoid of microtubules, and some microtubule endings terminate in regions devoid of F-actin accumulations characteristic of intrapodia. This may account for why we did not observe a significantly nonrandom association between microtubule endings and intrapodia in untreated growth cones. Nonetheless, our data are consistent with a causal linkage between microtubule polymerization and intrapodia.

DISCUSSION

We describe elemental features of a spontaneous, intralamellipodial, F-actin-rich structure that appears similar to those induced by pseudosubstrata (polycation-coated beads; Forscher *et al.*, 1992), intracellular pathogens (Cossart, 1995; Cudmore *et al.*, 1996), and to a lesser extent, vesicles in non-neuronal cells and cell extracts (Heuser *et al.*, 1992; Southwick *et al.*, 1997; Frischknecht *et al.*, 1999) and Arp2/3 spots in fibroblasts (Schafer *et al.*, 1998) (cf. Welch *et al.* 1997). Our data indicate that elongation of these spontaneous structures, termed intrapodia, depends absolutely on actin polymerization. We succeeded in altering the rate at which they occur by using drugs that target actin or microtubules. The direction of intrapodia elongation correlates with the direction of growth cone advance and intrapodial frequency is influenced by growth cone interaction with neurites. Still, the distribution of intrapodia, their transient nature, and the variability of their elongation patterns indicate that intrapodia are not primarily responsible for guiding growth cones or controlling their interaction with adjacent cells in vitro. In the three-dimensional matrices through which growth cones advance in vivo, however, we suspect that the microtubule–plasma membrane interactions that give rise to intrapodia in vitro represent a means by which microtubules may be able to stimulate F-actin-associated plasma membrane specializations independently of or interactively with extracellular cues.

Actin Polymerization Is Necessary for Intrapodial Elongation

Our light and electron microscopic analysis demonstrated that intrapodia contained more F-actin than surrounding regions of the lamellipodia. Of the filaments that we could analyze, 90% of those that were aligned parallel to the direction of elongation at the time of fixation had their barbed ends oriented toward the tip, consistent with a role for actin polymerization in pushing the tip forward. Cytochalasin and latrunculin B, two drugs that interfere with F-actin polymerization, blocked elongation of intrapodia. Cytochalasin has two effects on actin: at low concentrations it caps F-actin, and at higher doses it binds to monomers (Cooper, 1987). Given the difficulty of determining the intracellular concentration of cytochalasin and the effect of the cellular environment on its binding properties, we cannot extrapolate from the extracellular cytochalasin concentration which of the actin-binding properties is most responsible for the effects we describe (Cooper, 1987). Latrunculin B, a cell-permeant drug that does not bind to F-actin but facilitates depolymerization by binding G-actin (Spector *et al.*, 1989), had effects similar to those of cytochalasin B (our unpublished observations). This is consistent with the possibility that the impact of cytochalasin B results from its G-actin sequestering capability. These data demonstrate that actin polymerization is essential for intrapodia formation.

Most Intrapodial Leading Tips Are Likely to Be Associated with the Plasma Membrane

Intrapodia tips and tails are adjacent to and elevate the dorsal plasma membrane of lamellipodia. Thus, the plasma membrane at the front edge of the tip is approximately perpendicular to the direction of actin polymerization that is propelling the tip forward. No discrete structure (e.g., a vesicle) has been observed at the leading tips of intrapodia in growth cones (but see below). Furthermore, the association of intrapodia with elevated β_1-integrin staining is consistent with the possibility that intrapodia are linked to a membrane-associated protein. We cannot at this time rule out the possibility that the elevation in β_1-integrin staining and other F-actin-associated proteins (talin, α-actinin, and capping protein) is due to the increased fluorescence path length caused by

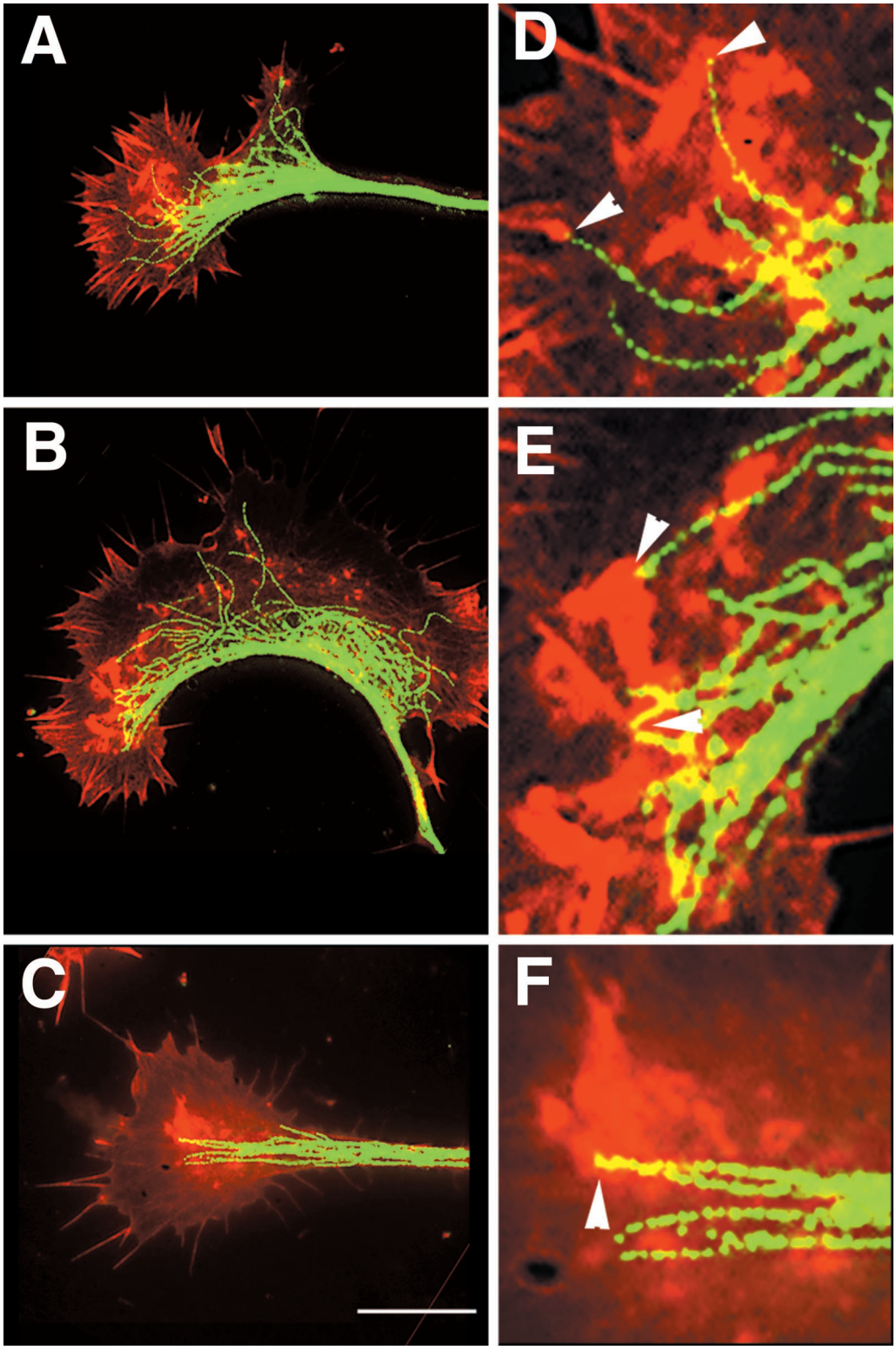

Figure 10. Microtubule endings are associated with intrapodial tails. Red corresponds to actin staining, green to microtubule staining. Growth cones in the presence or absence of microtubule-perturbing treatments were monitored during time-lapse DIC recordings and fixed during intrapodia formation. Arrowheads in D–F represent the initiation sites of intrapodia as determined before fixation during DIC observations. At high magnification, the microtubule staining sometimes appears discontinuous. Because similarly fixed samples prepared

Table 1. Microtubules are not randomly distributed with respect to intrapodia in the P domain

A Condition	B P domain area (μm^2)	C No. MT tips in P domain	D No. intrapodia	E No. MT tips ≤ 1 μm intrapodium	F p. MT tip ≤ 1 μm intrapodium (πD/B)	G p. $\geq$E colocal (1-ΣBin[$<$E,C])
Cntrl	52	6	2	2	0.12	0.16
Cntrl	52	9	2	1	0.12	0.68
Noc	112	5	3	2	0.08	0.06
Noc	152	8	4	3	0.08	0.03
Taxol	105	1	2	1	0.06	0.06
Taxol	61	1	1	1	0.05	0.05

In six growth cones fixed during the indicated conditions: Cntrl, untreated; Noc, after nocodazole washout; Taxol, after Taxol washin (A), We determined the area of the P domain (B), the number of microtubule (MT) tips in the P domain (C), the number of intrapodia in the P domain (D), the number of microtubule tips within 1 μm of the center of the initiation sites of the intrapodia (E), the probability that any particular microtubule would be found within 1 μm of the center of the initiation sites of the intrapodia (E), the probability that any particular microtubule would be found within 1 μm of an initiation site of any of the intrapodia if microtubules and intrapodia are distributed randomly throughout the P-domain (F) (can be viewed as the proportion of the area [B] occupied by D intrapodia initiation sites), and the probability of observing at least E colocalization events (G). This is determined by evaluating the binomial probability for less than E successes (colocalizations) for C trials (MT endings in the cone) given the probability determined in F for any particular trial (MT) to result in success (colocalization) and subtracting the chances for less than E successes from 1.0.

the sides of intrapodia. Presumably, cation-coated beads induce a specialization in the *Aplysia* growth cone plasma membrane to produce inductopodia (Forscher *et al.*, 1992), indicating that plasma membrane–based signaling is sufficient to induce intrapodia. All of the intracellular pathogens use either their own membrane surfaces (*Listeria*, *Shigella*, and *Rickettsia*) or cloak themselves in the host cell's intracellular membranes (Vaccinia virus), to provide a discrete organizer at the leading tip of the actin structure. In addition, there is evidence that the necessary actin-organizing proteins used by Vaccinia (Cudmore *et al.*, 1996) and *Listeria* (Friederich *et al.*, 1995), when present in the plasma membrane of infectable cells but separated from the pathogen, give rise to surface protrusions reminiscent of the protrusions induced by the intact pathogen. Finally, as noted by a reviewer, *Listeria* tails that are associated with the plasma membrane are more likely to contain long axial actin filaments (Sechi *et al.*, 1997) than those that are advancing through cytoplasm at a distance from the plasma membrane (Tilney *et al.*, 1992a,b), consistent with the possibility that the plasma membrane stabilizes or contributes to this component of filamentous actin tails. These data are consistent with the possibility that the plasma membrane contains the actin polymerization machinery that mediates intrapodia formation and that it may also influence the organization of actin filaments in the intrapodial tails.

A minority of intrapodia, those that arise from particles derived from the leading edge, are likely to be vesicle tipped. The behavior of these particles is unlike that of conventional intrapodia. In the example shown (Figure 1, D–K), the intrapodia-generating particle had elongated and shortened before the intrapodia type elongation (our unpublished observation). After the intrapodium elongation commenced, the particle appeared to split into two oppositely directed intrapodia. This would seem to suggest that opposite sides of a vesicle induce intrapodia. Note, however, that Schafer *et al.* (1998) have reported splitting of Arp3/capZ spots, which are evidently plasma membrane specializations. One of the intrapodia tips we described (Figure 1K) turned and advanced along linear elements (presumably microtubules). This is also difficult to explain for a plasma membrane specialization but not for a vesicle. There are reports of vesicle-tipped "actin rockets" that course through the cytoplasm in nonneuronal cell types (Heuser and Morisaki, 1992; Southwick *et al.*, 1997; Frischknecht *et al.*, 1999).

Cytochalasin B Washout Caused a Burst of Intrapodial Activity

Although the direct action of cytochalasin and latrunculin may be to sequester G-actin (Cooper, 1987), a

Figure 10 (cont). for EM show no evidence of microtubule fragmentation, we suspect that the discontinuities in staining are due to the antibody failing to bind a subset of antigen sites. If we used higher antibody concentrations, we obtained more continuous staining but also higher background. (A) Untreated growth cone fixed during intrapodia formation. (D) Digital zoom (4×) of a portion of the same cone shown in A. Some intrapodia are associated with microtubules (arrowheads). (B) After washout of nocodazole (0.33 μM), most of the intrapodia appear to have been initiated in the vicinity of microtubule endings. (E) Digital zoom of the intrapodia-rich area showing the close relationship between intrapodia (arrowheads) and microtubules. (C) After perfusion with medium containing 12 nM Taxol, intrapodia are initiated at sites rich in microtubule endings. (F) Digital zoom of the intrapodia-rich area (arrowheads) showing the relationship with microtubule ends. Bar, 18 μm.

consequence of these treatments is the formation of cytoplasmic swellings containing drug-resistant clusters of F-actin. Most of the intrapodial activity observed after cytochalasin washout emanated from these swellings. Verkhovsky *et al.* (1997) showed that F-actin in such clusters is organized into asters or crosses of antipolar filaments by myosin II. Thus, the F-actin is oriented with its barbed ends facing away from the center of the cluster. A subset of these barbed ends would be apposed to the dorsal plasma membrane and could facilitate the formation of or stabilize F-actin assembly-promoting complexes in the plasma membrane. Alternatively, we also observed that particles appeared to break away from the leading edge and become deposited in these swellings. These particles may contain preassembled complexes that could initiate intrapodia. As will be discussed below, these islands may form around microtubule endings, and the endings may be associated with intrapodia-initiating activity. In this light, it is interesting that plasma membrane tubules form after cytochalasin treatment in non-neuronal cells, and this tubulation depends on microtubules (van Deurs *et al.*, 1996). Note that although the effects of cytochalasin may not depend on its capping ability, the localization of capping protein along intrapodia suggests that capping protein is involved in tail assembly. Our impression is that capping protein staining is somewhat weaker at the leading tip, consistent with the possibility that intrapodia initiators uncap actin filaments locally or recruit or nucleate actin filaments. In summary, we propose that cytochalasin (latrunculin) treatment induces the formation of intrapodia initiators at cytoplasmic swellings, and that washout of the agent unleashes these initiators.

Microtubule Polymerization Promotes Intrapodia Formation

Intrapodia occasionally form in regions of lamellipodia remote from microtubules, but several lines of evidence indicate an intimate relationship between microtubule polymerization and intrapodia formation. Washout of nocodazole or addition of Taxol rapidly caused a spike in intrapodial activity, suggesting that microtubule polymerization within the growth cone stimulates intrapodia formation. This interpretation was supported by the finding that microtubule endings were often found at sites of intrapodia formation after the two treatments. The constitutive elevation of intrapodia frequency after overnight growth in nocodazole, paradoxical at first glance, is actually consistent with a role for microtubule endings in initiating intrapodia: there are more microtubules per unit length of marginal zone in chronically nocodazole-treated growth cones, and they tend to terminate just proximal to the marginal zone (Rochlin *et al.*, 1996), the site at which most intrapodia form. It is noteworthy that cytochalasin-resistant F-actin clusters are found at microtubule endings (Kelley *et al.*, 1996), and microtubules, like leading edges, are sites from which F-actin network assembly is initiated after washout of cytochalasin in *Aplysia* growth cones (Forscher and Smith, 1988). A correlation between microtubule endings and ruffle formation at the leading edge of non-neuronal cells has also been reported (Rinnerthaler *et al.*, 1988; Rosania and Swanson, 1996; Waterman-Storer *et al.*, 1999). The correlation between microtubule endings and intrapodia initiation sites, combined with the correspondence between microtubule polymerization and intrapodia initiation, supports involvement of microtubule endings or closely associated structures with induction of intrapodia.

Incorporating Microtubules, F-Actin, and the Plasma Membrane into a Model of Intrapodia Formation

We focus on the plasma membrane–associated intrapodia initiators because vesicle-tipped initiators are rare in growth cones and because they may simply represent ectopic leading edge fragments (endosomes) of limited importance in growth cone motility. We wish to address two questions raised by our observations: 1) how might microtubule polymerization induce intrapodia initiators in the overlying plasma membrane; and 2) why do microtubules induce intrapodia rather than filopodia?

Microtubules can influence the F-actin and plasma membrane by mechanical means, by virtue of transporting organelles (Dailey and Bridgman, 1991), or by enzymes associated with the microtubules. Polymerizing microtubule tips are able to drag endoplasmic reticulum tubules (Waterman-Storer *et al.*, 1995; Waterman-Storer and Salmon, 1998) and may therefore be able to push actin filaments encountered at the growing tip (perhaps via dynein activity, Waterman-Storer *et al.*, 1998). Although microtubules appear unable to resist the pressure of the constitutive retrograde flow of F-actin from the leading edge of lamellipodia (Waterman-Storer and Salmon, 1997; Suter *et al.*, 1998), they are able to grow into such regions, suggesting either an association of these microtubules with a non–rearward-moving F-actin population or the ability to polymerize without becoming cross-linked to the F-actin involved in the rearward flow. Microtubules appear to be drawn toward plasma membrane specializations associated with ventral surface integrin-based focal adhesions (Kaverina *et al.*, 1998) and sites of CAM cross-linking (Lin and Forscher, 1993; Suter *et al.*, 1998) and may therefore be capable of associating with a subpopulation of F-actin that is connected to plasma membrane tethers, perhaps via molecules that bind both microtubules and F-actin

(e.g., Heil-Chapdelaine *et al.*, 1998; Goode *et al.*, 1999). Polymerization of microtubules associated with this subpopulation of F-actin could lead to concentration or alignment of F-actin at the tip of the microtubule and thereby a concentration of the plasma membrane-associated tethers of these filaments, which in turn might accelerate cross-linking of these tethers. Cross-linking of CAMs by coated beads precedes and is necessary for inductopodia formation on the dorsal plasma membrane of *Aplysia* growth cones (Suter *et al.*, 1998) and is implicated as an initial step in the formation of actin–plasma membrane specializations at contact sites (Chrzanowska-Wodnicka and Burridge, 1996; Suter *et al.*, 1998). To date, however, there is little direct evidence supporting the possibility that microtubule polymerization moves F-actin in lamellipodia.

Microtubules are associated with a variety of enzyme activities, a subset of which are implicated in the regulation of the actin cytoskeleton (Kolodney and Elson, 1995; Best *et al.*, 1996; Nagata *et al.*, 1998). Small Ras-related GTPases cdc42, Rac, and Rho evidently control filopodial protrusion, ruffle formation and leading edge protrusion, and focal adhesion assembly in a variety of cell types (for review, see Hall, 1998), making them candidates for molecules through which microtubule polymerization may act. Several lines of evidence support a role for Rac1 in intrapodia initiation. Rac1 is implicated in ruffling and in pinocytosis (Ridley *et al.*, 1992), consistent with roles in both intrapodial F-actin assembly and the occasional formation of reverse phase organelles. Rac1 is also involved in the curvilinear, F-actin polymerization-based motility of spots of capZ/Arp3 in non-neuronal cells (Schafer *et al.*, 1998) and may be present in the *Listeria* F-actin tails (David *et al.*, 1998). In addition, it has been found to localize with microtubules in non-neuronal cells, and colchicine-induced microtubule depolymerization blocked ruffling caused by serum treatment, platelet-derived growth factor, and phorbol 12-myristate 13-acetate (Best *et al.*, 1996), each of which normally stimulates protrusive events via a pathway involving Rac1 (Ridley *et al.*, 1992; Nobes and Hall, 1995). Dominant negative Rac1 blocks the ruffling that normally accompanies microtubule repolymerization after nocodazole washout in fibroblasts (Waterman-Storer *et al.*, 1999). Recent observations implicate guanine nucleotide exchange factors, which bind to small GTPases and stimulate their activity, in the linkage of Rac to the polymerizing ends of microtubules (Ren *et al.*, 1998; Glavin *et al.*, 1999). One possibility suggested by these data is that microtubule polymerization delivers Rac1 to the plasma membrane and initiates protrusive-type actin assembly at a discrete site. If the site is not immobilized (e.g., via ECM attachment), it is propelled by the actin polymerization away from the microtubule, giving rise to an intrapodium.

Filopodia and ruffle-like sheets are capable of forming on the dorsal surface of our SCG growth cones (our unpublished observations); so why do intrapodia also form? We speculate that the tip specializations, the plasma membrane–linked protein complexes that induce F-actin assembly, are similar in intrapodia, filopodia, and ruffles, but levels of active F-actin-plasma membrane cross-linking proteins determine whether protrusion parallel to the direction of F-actin assembly (i.e., filopodia or ruffles) occurs at sites at which this F-actin assembly is stimulated. In the presence of high levels of cross-linking activity, recently assembled F-actin becomes linked to the plasma membrane. If the plasma membrane is "sticky," it is pulled toward the recently assembled F-actin and dragged forward by the tip, but if it is "slippery" (as in the case of intrapodia), the tip glides through the plasma membrane without pulling the plasma membrane along with it. The stickiness would be determined by the levels of the cross-linking proteins or their levels of activation (e.g., phosphorylation; Weed *et al.* 1998).

We have not determined the role of intrapodia in growth cone motility in vitro or in vivo. Nonetheless, the reproducible occurrence of intrapodia after washout of actin–monomer binding drugs or microtubule polymerization-stimulating drugs may provide an assay for determining the role of candidate signaling molecules in the early stages of formation of plasma membrane specializations involved in more typical forms of protrusion or the generation of adhesion specializations. Our finding that microtubule polymerization triggers intrapodia formation before (perhaps at the expense of) leading edge protrusion should encourage workers to incorporate this early, proximal event in models of microtubule-based motility alterations. Whether intrapodia occur in vivo is not known, but the frequency with which they occur in vitro suggests that the signaling events that underlie their initiation in vitro are active and significant in vivo.

ACKNOWLEDGMENTS

We thank Dr. John Cooper and Dr. Dorothy Schafer for comments on the manuscript and the gift of the anti-capping protein antibody. This work was supported by National Institutes of Health grant NS26510 (to P.C.B.).

REFERENCES

Beckerle, M.C. (1998). Spatial control of actin filament assembly: lessons from *Listeria*. Cell *95*, 741–748.

Berg, H.C., and Block, S.M. (1984). A miniature flow cell designed for rapid exchange of media under high-power microscope objectives. J. Gen. Microbiol. *130*, 2915–2920.

Bershadsky, A., Chausovsky, A., Becker, E., Lyubimova, A., and Geiger, B. (1996). Involvement of microtubules in the control of adhesion-dependent signal transduction. Curr. Biol. *6*, 1279–1289.

Bershadsky, A.D., Vaisberg, E.A., and Vasiliev, J.M. (1991). Pseudopodial activity at the active edge of migrating fibroblast is decreased after drug-induced microtubule depolymerization. Cell Motil. Cytoskeleton. *19*, 152–158.

Best, A., Ahmed, S., Kozma, R., and Lim, L. (1996). The Ras-related GTPase Rac1 binds tubulin. J. Biol. Chem. *271*, 3756–3762.

Bridgman, P.C., and Dailey, M.E. (1989). The organization of myosin and actin in rapid frozen nerve growth cones. J. Cell Biol. *108*, 95–109.

Chrzanowska-Wodnicka, M., and Burridge, K. (1996). Rho-stimulated contractility drives the formation of stress fibers and focal adhesions. J. Cell Biol. *133*, 1403–1415.

Cooper, J.A. (1987). Effects of cytochalasin and phalloidin on actin. J. Cell Biol. *105*, 1473–1478.

Cooper, J.A. (1991). The role of actin polymerization in cell motility. Annu. Rev. Physiol. *53*, 585–605.

Cossart, P. (1995). Actin-based bacterial motility. Curr. Opin. Cell Biol. *7*, 94–101.

Cramer, L.P., Mitchison, T.J., and Theriot, J.A. (1994). Actin-dependent motile forces and cell motility. Curr. Opin. Cell Biol. *6*, 82–86.

Cudmore, S., Reckmann, I., Griffiths, G., and Way, M. (1996). Vaccinia virus: a model system for actin-membrane interactions. J. Cell Sci. *109*, 1739–1747.

Dailey, M.E., and Bridgman, P.C. (1991). Structure and organization of membrane organelles along distal microtubule segments in growth cones. J. Neurosci. Res. *30*, 242–258.

Dailey, M.E., and Bridgman, P.C. (1993). Vacuole dynamics in growth cones: correlated EM and video observations. J. Neurosci. *13*, 3375–3393.

David V., Gouin, E., Van Troys, M., Grogan, A., Segal, A.W., Ampe, C., and Cossart, P. (1998). Identification of cofilin, coronin, Rac and capZ in actin tails using a *Listeria* affinity approach. J. Cell Sci. *111*, 2877–2884.

Evans, L.L., and Bridgman, P.C. (1995). Particles move along actin filament bundles in nerve growth cones. Proc. Natl. Acad. Sci. USA *92*, 10954–10958.

Forscher, P., Lin, C.H., and Thompson, C. (1992). Novel form of growth cone motility involving site-directed actin filament assembly. Nature *357*, 515–518.

Forscher, P., and Smith, S.J. (1988). Actions of cytochalasins on the organization of actin filaments and microtubules in a neuronal growth cone. J. Cell Biol. *107*, 1505–1516.

Friederich, E., Gouin, E., Hellio, R., Kocks, C., Cossart, P., and Louvard, D. (1995). Targeting of *Listeria* monocytogenes ActA protein to the plasma membrane as a tool to dissect both actin-based cell morphogenesis and ActA function. EMBO J. *14*, 2731–2744.

Frischknecht, F., Cudmore, S., Moreau, V., Reckmann, I., Rottger, S., and Way, M. (1999). Tyrosine phosphorylation is required for actin-based motility of vaccinia but not *Listeria* or *Shigella*. Curr. Biol. *9*, 89–92.

Glavin, J.A., Whitehead, I., Bagrodia S., Kay, R., and Cerione, R.A. (1999). The Dbl-related protein, Lfc, localizes to microtubules and mediates the activation of Rac signaling pathways in cells. J. Biol. Chem. *274*, 2279–2285.

Goode, B.L., Wong, J.J., Butty, A-C., Peter, M., McCormack, A.L., Yates, J.R., Drubin, D.G., and Barnes, G. (1999). Coronin promotes the rapid assembly of and cross-linking of actin filaments and may link the actin and microtubule cytoskeletons in yeast. J. Cell Biol. *144*, 83–98.

Hall, A. (1998). Rho GTPases and the actin cytoskeleton. Science *279*, 509–514.

Heil-Chapdelaine, R.A., Tran, N.K., and Cooper, J.A. (1998). The role of *Saccharomyces cerevisiae* coronin in the actin and microtubule cytoskeletons. Curr. Biol. *8*, 1281–1284.

Heinzen, R.A., Hayes, S.F., Peacock, M.G., and Hackstadt, T. (1993). Directional actin polymerization associated with spotted fever group *Rickettsia* infection of Vero cells. Infect. Immun. *61*, 1926–1935.

Heuser, J.E., and Morisaki, J.H. (1992). Time-lapse video microscopy of endosomal "rocketing" in La/Zn treated cells. Mol. Biol. Cell *3*(suppl), 172a (Abstract).

Honer, B., Citi, S., Kendrick-Jones, J., and Jockusch, B.M. (1988). Modulation of cellular morphology and locomotory activity by antibodies against myosin. J. Cell Biol. *107*, 2181–2189.

Jordan, M.A., Toso, R.J., Thrower, D., and Wilson, L. (1993). Mechanism of mitotic block and inhibition of cell proliferation by Taxol at low concentrations. Proc. Natl Acad. Sci. USA *90*, 9552–9556.

Katoh, K., Hammar, K., Smith, P.J., and Oldenbourg, R. (1999). Birefringence imaging directly reveals architectural dynamics of filamentous actin in living growth cones. Mol. Biol. Cell *10*, 197–210.

Kaverina, I., Rottner, K., and Small, J.V. (1998). Targeting, capture, and stabilization of microtubules at early focal adhesions. J. Cell Biol. *142*, 181–190.

Kelley, C.A., Sellers, J.R., Gard, D.L., Bui, D., Adelstein, R.S., and Baines, I.C. (1996). *Xenopus* nonmuscle myosin heavy chain isoforms have different subcellular localizations and enzymatic activities. J. Cell Biol. *134*, 675–687.

Kolodney, M.S., and Elson, E.L. (1995). Contraction due to microtubule disruption is associated with increased phosphorylation of myosin regulatory light chain. Proc. Natl. Acad. Sci. USA *92*, 10252–10256.

Lewis, A., and Bridgman, P.C. (1992). Nerve growth cone lamellipodia contain two populations of actin filaments that differ in organization and polarity. J. Cell Biol. *119*, 1219–1243.

Lin, C., and Forscher, P. (1993). Cytoskeletal remodeling during growth cone–target interactions. J. Cell Biol. *121*, 1369–1383.

Lin, C.H., Espreafico, E.M., Mooseker, M.S., and Forscher, P. (1996). Myosin drives retrograde F-actin flow in neuronal growth cones. Neuron *16*, 769–782.

Mitchison, T., and Kirschner, M. (1988). Cytoskeletal dynamics and nerve growth. Neuron *1*, 761–772.

Nagata, K., Puls, A., Futter, C., Aspenstrom, P., Schaefer, E., Nakata, T., Hirokawa, N., and Hall, A. (1998). The MAP kinase kinase kinase MLK2 colocalizes with activated JNK along microtubules and associates with kinesin superfamily motor KIF3. EMBO J. *17*, 149–158.

Nobes, C.D., and Hall, A. (1995). Rho, Rac, and cdc42 GTPases regulate the assembly of multimolecular focal complexes associated with actin stress fibers, lamellipodia, and filopodia. Cell *81*, 53–62.

Oster, G.F., and Perelson, A.S. (1987). The physics of cell motility. J. Cell Sci. Suppl. *8*, 35–54.

Ren, Y., Li, R., Zheng, Y., and Busch, H. (1998). Cloning and characterization of GEF-H1, a microtuble-associated guanine nucleotide exchange factor for Rac and Rho GTPases. J. Biol. Chem. *273*, 34954–34960.

Ridley, A.J., Paterson, H.F., Johnston, C.L., Diekmann, D., and Hall, A. (1992). The small GTP-binding protein Rac regulates growth factor-induced membrane ruffling. Cell *70*, 401–410.

Rinnerthaler, G., Geiger, B., and Small, J.V. (1988). Contact formation during fibroblast locomotion, involvement of membrane ruffles and microtubules. J. Cell Biol. *106*, 747–760.

Rochlin, M.W., Itoh, K.I., Adelstein, R.S., and Bridgman, P.B. (1995). Localization of myosin II A and B isoforms in cultured neurons. J. Cell Sci. *108*, 3661–3670.

Rochlin, M.W., Wickline, K.M., and Bridgman, P.C. (1996). Microtubule stability decreases axon elongation but not axoplasm production. J. Neurosci. *16*, 3236–3246.

Rosania, G.R., and Swanson, J.A. (1996). Microtubules can modulate pseudopod activity from a distance inside macrophages. Cell Motil. Cytoskeleton *34*, 230–245.

Schafer, D.A., Welch, M.D., Machesky, L.M., Bridgman, P.C., Meyer, S.M., and Cooper, J.A. (1998). Visualization and molecular analysis of actin assembly in living cells. J. Cell Biol. *143*, 1919–1930.

Schliwa, M., Euteneuer, U., Bulinski, J.C., and Izant, J.G. (1981). Calcium lability of cytoplasmic microtubules and its modulation by microtubule-associated proteins. Proc. Natl. Acad. Sci. USA *78*, 1037–1041.

Sechi, A.S., Wehland, J., and Small, J.V. (1997). The isolated comet tail pseudopodium of listeria monocytogenes: a tail of two actin filament populations, long and axial and short and random. J. Cell Biol. *137*, 155–167.

Smith, S.J. (1988). Neuronal cytomechanics: the actin-based motility of growth cones. Science *242*, 708–715.

Southwick, F.E., Heuser, J.E., Beckerle, M.C., Shen, P., and Purich, D.L. (1997). Actin-based endosomal rocketing involves zyxin, VASP, and profilin. Mol. Biol. Cell *8*(suppl), 169a (Abstract).

Spector, I., Shochet, N.R., Blasberger, D., and Kashman, Y. (1989). Latrunculins—novel marine macrolides that disrupt microfilament organization and affect cell growth: I. Comparison with cytochalasin D. Cell Motil. Cytoskeleton *13*, 127–144.

Suter, D.M., Errante, L.D., Belotserkovsky, V., and Forscher, P. (1998). The Ig superfamily cell adhesion molecule, apCAM, mediates growth cone steering by substrate-cytoskeletal coupling. J. Cell Biol. *141*, 227–240.

Svitkina, T.M., and Verkhovsky, A.B. (1995). Improved procedures for electron microscopic visualization of the cytoskeleton of cultured cells. J. Struct. Biol. *115*, 290–303.

Svitkina, T.M., Vrekhovsky, A.B., McQuade, K.M., and Borisy, G.G. (1997). Analysis of the actomyosin II system in fish epidermal keratocystes-mechanism of cell body translocation. J. Cell Biol. *139*, 397–415.

Tanaka, E., Ho, T., and Kirschner, M.W. (1995). The role of microtubule dynamics in growth cone motility and axonal growth. J. Cell Biol. *128*, 139–155.

Tanaka, E., and Kirschner, M.W. (1991). Microtubule behavior in the growth cones of living neurons during axon elongation. J. Cell Biol. *115*, 345–363.

Tanaka, E., and Kirschner, M.W. (1995). The role of microtubules in growth cone turning at substrate boundaries. J. Cell Biol. *128*, 127–137.

Tanaka, E., and Sabry, J. (1995). Making the connection: cytoskeletal rearrangements during growth cone guidance. Cell *83*, 171–176.

Tilney, L.G., DeRosier, D.J., and Tilney, M.S. (1992a). How *Listeria* exploits host cell actin to form its own cytoskeleton. I. Formation of a tail and how that tail might be involved in movement. J. Cell Biol. *118*, 71–81.

Tilney, L.G., DeRosier, D.J., Weber, A., and Tilney, M.S. (1992b). How *Listeria* exploits host cell actin to form its own cytoskeleton. II. Nucleation, actin filament polarity, filament assembly, and evidence for a pointed end capper. J. Cell Biol. *118*, 83–93.

van Deurs, B., von Bülow, F., Vilhardt, F., Kaae Holm, P., and Sandvig, K. (1996). Destabilization of plasma membrane structure by prevention of actin polymerization. Microtubule-dependent tubulation of the plasma membrane. J. Cell Sci. *109*, 1655–1665.

Vasiliev, J.M., and Gelfand, I.M. (1976). Effects of colcemid on morphogenetic processes and locomotion of fibroblasts. In: Cell Motility, ed. R. Goldman, T. Pollard, and J. Rosenbaum, Cold Spring Harbor, NY: Cold Spring Harbor Laboratory, 279–304.

Verkhovsky, A.B., Svitkina, T.M., and Borisy, G.G. (1997). Polarity sorting of actin filaments in cytochalasin-treated fibroblasts. J. Cell Sci. *110*, 1693–1704.

Verkhovsky, A.B., Svitkina, T.M., and Borisy, G.G. (1999). Self-polarization and directional motility of cytoplasm. Curr. Biol. *9*, 11–20.

Waterman-Storer, C.M., Gregory, J., Parsons, S.F., and Salmon, E.D. (1995). Membrane/microtubule tip attachment complexes (TACs) allow the assembly dynamics of plus ends to push and pull membranes into tubulovesicular networks in interphase *Xenopus* egg extracts. J. Cell Biol. *130*, 1161–1169.

Waterman-Storer, C.M., and Salmon, E.D. (1997). Actomyosin-based retrograde flow of microtubules in the lamella of migrating epithelial cells influences microtubule dynamic instability and turnover and is associated with microtubule breakage and treadmilling. J. Cell Biol. *139*, 417–434.

Waterman-Storer, C.M., and Salmon, E.D. (1998). Endoplasmic reticulum membrane tubules are distributed by microtubules in living cells using three distinct mechanisms. Curr. Biol. *8*, 798–806.

Waterman-Storer, C.M., Salmon, E.D., and Bement, W.M. (1998). Microtubules modify actin networks in *Xenopus* egg extracts by dynein-dependent pushing and pulling of actin bundles. Mol. Biol. Cell *9*(suppl), 140a (Abstract).

Waterman-Storer, C.M., Worthylake, R.A., Liu, B.P., Burridge, K., and Salmon, E.D. (1999). Microtubule growth activates Rac1 to promote lamellipodial protrusion in fibroblasts. Nat. Cell Biol. *1*, 45–50.

Weed, S.A., Du, Y., and Parsons, J.T. (1998). Translocation of cortactin to the cell periphery is mediated by the small GTPase Rac1. J. Cell Sci. *111*, 2433–2443.

Welch, M.D., DePace, A.H., Verma, S., Iwamatsu, A., and Mitchison, T.J. (1997). The human arp2/3 complex is composed of evolutionarily conserved subunits and is localized to cellular regions of dynamic actin filament assembly. J. Cell Biol. *138*, 375–384.

Williamson, T., Gordon-Weeks, P.R., Schachner, M., and Taylor, J. (1996). Microtubule reorganization is obligatory for growth cone turning. Proc. Natl. Acad. Sci. USA *93*, 15221–15226.

Zhukarev, V., Ashton, F., Sanger, J.M., and Shuman, H. (1995). Organization and structure of actin filament bundles in *Listeria*-infected cells. Cell Motil. Cytoskeleton *30*, 229–246.